

## Concentric Rings K-space Trajectory for Hyperpolarized $^{13}\text{C}$ MRSI

Wenwen Jiang<sup>1</sup>, Michael Lustig<sup>2</sup>, and Peder Larson<sup>3</sup>

<sup>1</sup>UC Berkeley | UCSF Graduate Group in Bioengineering, Berkeley, California, United States, <sup>2</sup>Electrical Engineering, University of California, Berkeley, Berkeley, California, United States, <sup>3</sup>Radiology and Biomedical Imaging, University of California, San Francisco, San Francisco, CA, United States

**Target audience:** MR pulse sequence design, Hyperpolarized  $^{13}\text{C}$  MRI, spectroscopic imaging scientists and engineers

**Purpose:** The powerful feature of hyperpolarized  $^{13}\text{C}$  MR metabolic imaging<sup>1</sup> is that it can not only support the initial diagnosis of cancer but also can monitor its progress in terms of staging, restaging, treatment response, and identification of recurrence. However, the short-lived effect of hyperpolarization requires rapid and robust imaging techniques. Echo-planar-based spectroscopic imaging (EPSI) techniques are popular for acceleration in MRSI. The spectral bandwidth (SBW) of EPSI is limited by slew rate. System imperfections will induce undesirable ghosting artifacts for EPSI. Concentric rings k-space sampling<sup>2,3</sup> has advantages of reduced slew rate, acquisition timesaving, and robustness to system delay and eddy currents, providing a powerful alternative for accelerating MRSI.

**Theory:** Concentric rings trajectories have smooth gradients waveforms, which are less demanding on the gradient amplifiers than for EPSI, given the same prescription. Each ring covers 4 quadrants in spatial k-space, which halves the total scan time. The symmetric property of the rings makes it robust to timing delays, which only result in rotation of the image. And its SNR efficiency is a constant of 87%<sup>4,5</sup> (the analyses are shown in Fig.1). Additionally, this non-Cartesian trajectory allows better control of variable density sampling and theoretically fits much better with parallel imaging and compressed sensing accelerations.<sup>6</sup>

**Methods:** Time-optimal gradient waveforms were designed based on Hargreaves's work<sup>7</sup> using MATLAB and CVX toolbox.<sup>8</sup> Trajectory was designed for the  $3.6 \times 3.6 \text{ mm}^2$  spatial resolution,  $8 \times 8 \text{ cm}^2$  FOV and 500Hz SBW, 10Hz spectral resolution, as Fig.2 shows. The following acquisition parameters were used: TE/TR=120ms/200ms, 11 phase-encoded excitations with a progressive flip angle, resulting in a total scan time of 2.32s. The readout gradients were implemented in an adiabatic spin-echo sequence on a GE Signa 3T scanner. All the data were processed offline using MATLAB and SIVIC software (UCSF, San Francisco, CA). We performed normal rat experiments at 27 seconds after an injection of 2.2 mL of 100 mM hyperpolarized [ $^{13}\text{C}$ ] pyruvate (using an Oxford Instruments HyperSense polarizer).

**Results and Discussion:** In the *in vivo* hyperpolarized  $^{13}\text{C}$  MRSI study, we applied concentric rings sequence to sample the k-space data and the NUFFT algorithm<sup>9</sup> for reconstruction. The results are shown in Fig.3. We also used the same sequence to image a GE proton phantom at 1mm resolution as reference. At that resolution, we noticed image artifacts due to concomitant gradients. These have little effect for the resolution of our  $^{13}\text{C}$  images, but if higher resolution is desired they should be corrected for.

**Conclusion:** Our preliminary results demonstrate the potential of using concentric rings in hyperpolarized  $^{13}\text{C}$  MRSI for a two-fold acceleration of EPSI.

### References:

[1] Kurhanewicz J, et al. Neoplasia 2011; Nov: VOL.13, NO.2. [2] Wu. H. [D] Stanford University, 2009. [3] Furuyama J, et al. MRM 2012; 67:1515–1522. [4] Cunningham CH, et al. MRM 2005; 54:1286–1289. [5] Tsai C, Nishimura D. MRM 2000; 43:452–458. [6] Hu S, et al. JMR 2008 June; 192(2): 258–264. [7] Hargreaves BA, et al. MRM 2004; 51:81–92. [8] CVX Research, Inc. <http://cvxr.com/cvx>, September 2012. [9] Fessler J, et al. IEEE TRANS 2003;Feb: VOL. 51, NO. 2

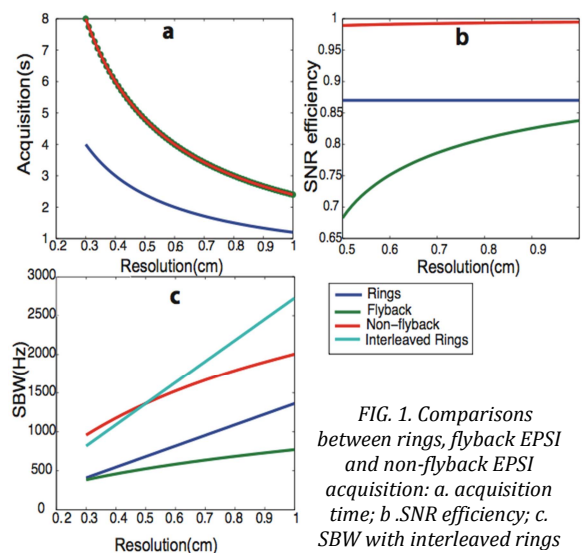


FIG. 1. Comparisons between rings, flyback EPSI and non-flyback EPSI acquisition: a. acquisition time; b. SNR efficiency; c. SBW with interleaved rings

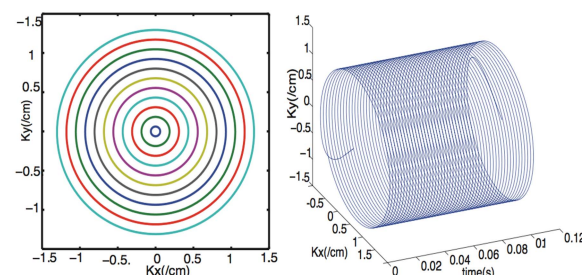


FIG. 2. (left) Spatial k-space coverage of all rings; (right) A single ring retraced over time

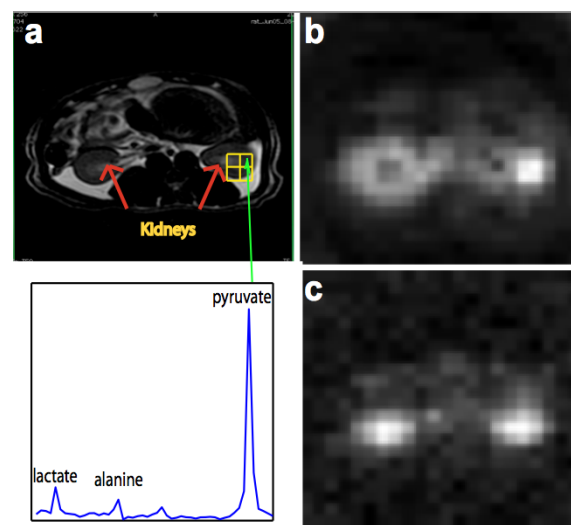


FIG. 3. In vivo results on a normal rat (axial slice): a. proton image; b.  $^{13}\text{C}$  pyruvate image; c.  $^{13}\text{C}$  lactate image